INFLUENCE OF SOME AGGREGATES OF DIVERSE NATURE ON THE CHARACTERISTICS OF LIME MORTARS

Fábio Botelho Costa
(fabio.b.costa@tecnico.ulisboa.pt)

Instituto Superior Técnico, Portugal

May 2017

Abstract.

Lime-based rendering mortars applicated on old buildings contribute to the better characteristics of compatibility in relation to cement mortars. Fine aggregates are main constituents of mortars with a great influence on their behavior. The purpose of this work is to study the influence of aggregate nature on the physical and mechanical behavior of lime mortars. To this end, three lime mortars with a volumetric proportion of 1:3 (lime:aggregate) were produced with three types of fine aggregates, namely the traditional quartzitic sands, calcareous sands and volcanic sands. The quartzitic sands have been the most used aggregates in rendering mortars, the calcareous sands can improve the mechanical resistance of lime mortars and the volcanic sands are widely used in places where they are abundant, as in the case of some Portuguese islands of Azores. Mortars were produced in 4x4x16cm prismatic specimens and applied as renders on a small prototype masonry wall. There was a highest mechanical strength found in the mortars with the carbonate aggregates but similar water transport properties to those of quartzitic aggregate mortars. The volcanic sand mortars obtained the lowest mechanical strength and the highest permeability.

Keywords: Aerial lime; renders; walls of old buildings; quartzitic sands; calcareous sands; volcanic sands.

1 INTRODUCTION

Aerial lime was the main binder used in masonry mortars for centuries. Many of the existing constructions before and after he 19th century were built with this technology. The preservation of these buildings justifies the research on lime mortars technology and the pursue for new and better solutions for the replacement of ancient mortars. Therefore, the aerial lime should be the best intervention for the conservation of ancient buildings [1,2,3]. It is expected that the replacement mortars have the same properties, or that they are as similar as possible, to the original mortars. These properties are, among others, their capacity to water absorption and at, the same time, their drying capacity [4,5,6].

The natural aggregates presented in the mortars are the constituents in higher volume and, therefore, will influence not only their physical and mechanical behavior, but also their fresh and hardened state [7,8,9,10].

Some studies reveal that the influence of carbonate aggregates lead to a higher mechanical strength than traditional quartzitic sands, even though these are more commonly used [11,12,13,14,15]. Nogueira (2016) and Santos et al. (2016) proved that mortars with the carbonate aggregates allowed higher compressive strength up to 50-60% comparing to traditional mortars. The aggregate-paste interface transition zone (*ITZ*) is a factor that benefits the carbonate sands mortars [11,14,15,16].

Despite these studies, further investigation must be done, not only in this field but also in mortars with volcanic aggregates. Although these types of natural aggregates are abundant and used in the archipelago of the Azores, one should study the behavior of this type of aggregate.

The main aim of this work is to evaluate the influence of aggregate nature on the physical and mechanical behavior of lime mortars. In order to accomplish this, Three lime-based mortars

with a lime/aggregate ratio of 1:3 (v:v) and the same water/lime ratio, produced with three types of fine aggregates possible to be used in Portugal, a traditional quartzitic sand, a carbonate sand and a volcanic sand. All three mortars were tested for 120 days of curing age to ensure that they were presented completely carbonated.

While performing laboratory work, the three types of aggregates had in common the grading curves. The quartzitic and calcareous sands were modified to attain grading curves similar to that of the volcanic sands.

Mortars were characterized in terms of their main physical and mechanical properties evaluated in 4x4x16cm prismatic specimens (porosity and density, compressive and flexural strength, ultrasonic-pulse velocity, dynamic modulus of elasticity, water absorption by immersion, water absorption by capillarity, water vapor permeability and drying behavior). They were also applied as renders on a small prototype masonry wall and their behavior was analyzed by through *in-situ* tests (pull-off, drilling resistance, superficial hardness and Karsten pipe).

The mortars were evaluated and compared to each other, as also established the relative performance of specimens and renders.

2 EXPERIMENTAL WORK

2.1 Materials

The binder used was the aerial lime type CL90 in accordance with EN 459-1: 2001. The bulk density of lime is 600 kg/m^3 and the particle density is 2200 kg/m^3.

The natural aggregates used were a quartzitic sand, a carbonate sand, a volcanic sand. The grain size distribution of quartzitic and carbonate sands were adjusted to resemble the same grading curve as the volcanic sand, which was set as the reference aggregate. The grading curve of quartzitic sand was composed of equal proportions of 0/2 and 0/4 commercial sands (Figure 1).

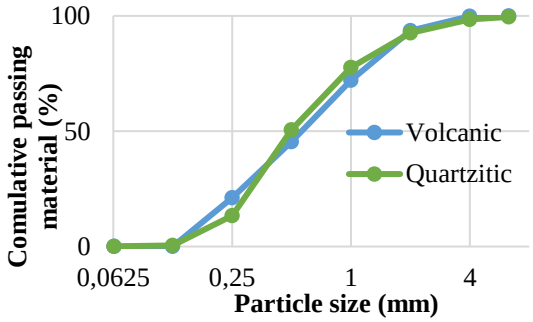

Figure 1 – Grading curves of aggregates [EN 933-1:2000]

The quartzitic sands are natural washed-sands composed of quartz and feldspar with sub-angular to sub-rounded particles. The volcanic sand is non-washed with dimension of 0/2 and consists mainly of fragments of pyroclastic rocks that resulted from the consolidation of volcanic ash. It also contains basaltic and trachytic rocks particles that appeared in the transport process. The particles are mostly rounded, between the quartzitic and carbonate sands configuration. Both volcanic and quartzitic sands are siliceous nature. The carbonate sand is not showed on Figure 1 but it was also graduated in the same way as volcanic sand grading curve by the diverse size fractions from the marble crushing. The particles are mainly angular, which results from the manufacturing process. It´s also non-washed.

The packing density was estimated in terms of ρ (dried density) and ρ_l (loose bulk density), according to the equation [17]:

$$\phi = \frac{V_s}{Vs+Vv} = \frac{\rho_l}{\rho}(\ ) \quad (1)$$

Table 1 summarizes the physical properties of the aggregates.

Table 1 - Physical characterization of aggregates

Property	Aggregate			
	Quartzitic		Calcareous	Volcanic
	Fine Sand	Coarse Sand		
Water absorption 24h (%)[1]	0,3	0,4	0,2	2,0
Dried density (kg/m^3)[1]	2560	2560	2720	2300
Loose Bulk density (kg/m^3)[2]	1510	1530	1580	1240
Packing density ( )	0.59	0.60	0.58	0.54
Volume de vazios (%)[2]	41	40,2	41,9	46,1

([1]) EN 1097-6 ([2]) EN 1097-3

2.2 Lime mortars

The experimental program consisted in producing three mortars with different aggregates and a water/lime ratio of 1.55 (w:w), in order to isolate the effect of each of the aggregate in the several properties studied. To simplify, from now on, the aggregate´s designations of the mortars with quartzitic, carbonate and volcanic sands will be Q, C and V-mortars, respectively.

The mortars were prepared according to the EN 196-1:2005. Prisms were molded in 40 x 40 x 160 mm^3 and renders were applied in a stone masonry prototype with about (l x h x t) 120 x 90 x 40 cm^3 made of natural limestone blocks and lime mortar (Figure 2a). The mortars were applied on the two sides of the wall, one of them was covered with two adjacent panels of around (l x h) 60 x 90 cm^2 each (Figure 2b) and the other covered with Q-mortar of around (l x h) 120 x 80 cm^2.

(a) **(b)**

Figure 2 – (a) Stone masonry prototype; (b) Renders of C and V-mortar

The mortars manifested different consistencies for the same water/lime ratio due of the diverse nature and shape of the aggregates particles. V-mortar was the least fluid and workability, however extra water was added to this mixture there was higher water absorption of the aggregates (Table 1). According to the table flow test of EN 1015-3:1999, the results of flow are 196 mm, 151 mm and 132 mm from Q, C and V-mortar, respectively.

2.3 Tests characterization

The characterization in prisms and renders involved physical and mechanical tests. Before that, the prisms were kept in a room with environmental conditions (T=19±2°C and RH=60±5%) and the renders in the environmental conditions of laboratory. Both prisms and renders were tested for 120 days. The prisms that were used in water absorption tests were previously dried for about 72 hour in an oven at 60±5°C.

The list of tests on hardened state and their specifications documents, along with the lab equipment are presented in Table 2.

Table 2 - Tests on hardened state mortars

Specimens	Test	Standard	Lab equipment
Prisms	Porosity and bulk density	RILEM I.1 & I.2	Sealed container and vacuum pump
	Compressive and flexural strenght	EN 1015-11	Sneider universal, model D-7940
	Ultrasonic pulse velocity	EN 12504-4	PUNDIT from Proceq
	Dynamic modulus of elasticity	ASTM E 1876-01	GrindoSonic E-modulus
	Water absorption by immersion	LNEC E394	–
	Water capillary absorption	EN 1015-18	–
	Water vapour permeability	RILEM II.2; [18,19]	–
	Drying behaviour	RILEM II.5	–
Renders	Drilling resistance	–	SINT Technology DRMS
	Surface hardness	–	Schmidt pendulum sclerometer type PT
	Pull-off	EN 1015-12	Pull-off equipment
	Water absorption by Karsten pipe	RILEM II.4	Karsten tube

The water absorption by immersion gives the volume of water absorbed by the specimen during 48 hour at atmospheric pressure. The water vapour permeability based on an operation which enables a unidirectional flux of water vapour crossing the material specimen. The flux is due to a pressure difference (external environment RH≅75%; inside the cell RH≅10%) that is created between both sides of the specimen, increasing its weight. The dimensions of specimens are (l x h x t) 4 x 4 x 2 cm were sealed with an epoxy resin (Sikadur® 32,5N, Sika) to improve unidirectional water vapour flux.

In the drying behavior test, the specimens are half-parts of prisms (around 4 x 4 x 6 cm), with the lateral faces sealed with epoxy resin (Sikadur® 32,5N, Sika) and bottom face with polyethylene film, leaving the top face exposed to allow the evaporation to go in one direction. The specimens were immersed in water for 48 hours and immediately after the drying test began in a room with environmental conditions (T=19±2°C and RH=60±5%).

The drilling resistance consists of making a small hole in the surface of the prisms and the renders by a drill fitted with a load cell, in order to determine the resistance by drilling (100 rpm and 40 mm/min) through the depth.

3 RESULTS AND DISCUSSION

3.1 Characterization in prisms

3.1.1 Mechanical properties

The results of mechanical properties are showed in Table 3.

Table 3 - Mechanical properties

Mortar	f_c[1] (MPa)	f_f[2] (MPa)	F_d[3] (N)	UPV[4] (m·s^{-1})	E_d[5] (GPa)
Q	0.79±0.01	0.33±0.03	3.9±0.6	1585±40	3.8±0.3
C	0.98±0.04	0.41±0.02	7.4±0.6	1540±30	3.7±0.3
V	0.77±0.01	0.25±0.01	3.2±0.5	1120±10	1.4±0.1

[1]compressive strength; [2]flexural strength; [3]drilling resistance; [4]ultrasonic pulse velocity; [5]dynamic modulus of elasticity (mean and standard deviation).

It's important to mention that the mechanical resistance reached of the three mortars were low. However, the C-mortar showed better results in the destructive tests, such as f_c, f_f and F_d, while V-mortar obtained the lowest values in all of properties mentioned in Table 3. Depending on the property, the C-mortar values were 24-90 % and 26-131 % higher than those of Q and V-mortars, respectively.

The lowest strength of the V-mortar can't be attributed only to its higher void content and to its worst workability, but also to the surface flexural failure. This surface was more regular in relation to the others mortars, because it developed while going through the volcanic aggregate

particles, which conditioned the decrease of its strength (Figure 3c). This effect must have been the main responsible for the reduction of the flexural strength, since the compressive strength results are closed to those of Q-mortar. In fact, in compression, aggregates are benefited by the confinement effect that increases their mechanical strength [20].

It's clearly demonstrated by several authors [11,14,15,21] that mortars produced with carbonate aggregates develop higher strength than mortars produced with quartzitic aggregates. This may be explained both by the connexion of the carbonate aggregates (where failure surface passes through the paste, Figure 3b) and the chemistry that exists between the carbonate aggregates and the lime paste that causes more regular microstructure in such area [11,12]. The higher angularity of carbonate aggregates is also in their favour. Contrary, the failure surface in Q-mortar tended to path preferentially through the *ITZ*, showing aggregate particles (Figure 3a).

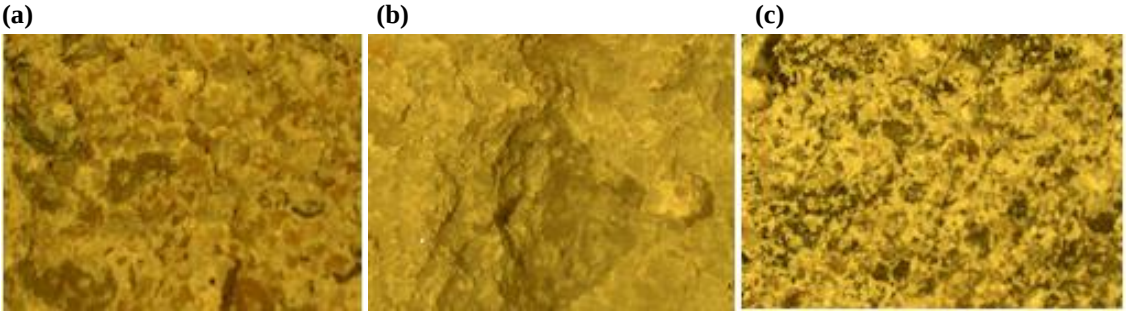

(a) Q-mortar: irregular surface showing aggregate particles with clean surface without significant paste;
(b) C-mortar: homogeneous irregular failure surface with aggregate particles covered by paste;
(c) V-mortar: more regular failure surface with visible broken aggregate particle.

Figure 3 – Flexural failure surface of mortar specimens

In what regards the non-destructive tests, such as the ultrasonic pulse velocity (*UPV*) and dynamic modulus of elasticity (E_d), the same conclusions are not drawn from the others properties mentioned above, except for the V-mortar that continues to have lowest values. The V-mortar showed higher paste volume and lower stiffness of their aggregates.

On the other hand, Q-mortar had slightly higher *UPV* and E_d than C-mortar (Table 3 and Figure 4). Therefore, this difference can be explained by the stiffness and density of each mortar, which in this case, the Q-mortar had more stiffness of their aggregates and lower paste volume (highest aggregate packing density, Table 1).

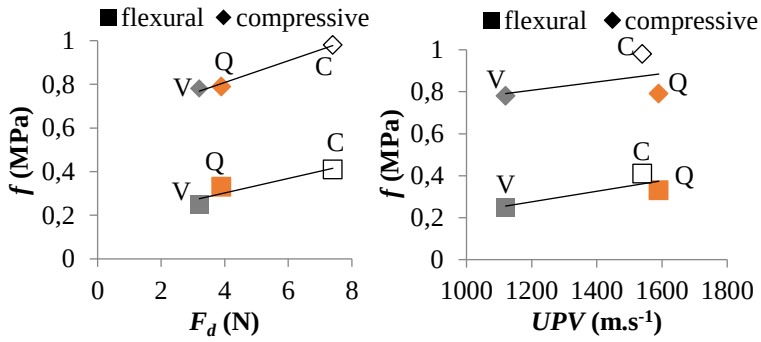

Figure 4 - Relationships between compressive and flexural strength and drilling resistance (left) and ultrasonic pulse velocity (right)

In homogeneous materials, *UPV* can be expressed in terms of E_d, ρ (dried density) and ν_d (dynamic Poisson coefficient) according to the expression (2). The *UPV* shows the same behavior as E_d [22,23].

$$UPV = \sqrt{\frac{E_d}{\rho} \times \frac{(1-v_d)}{(1+v_d)\times(1-2v_d)}} \quad (2)$$

3.1.2 Physical properties

The results of physical properties concerning porosity and pore structure are presented in Table 4.

Table 4 - Physical properties

Mortar	P_w [1] (%)	ρ_b [2] (kg/m^3)	ρ [3] (kg/m^3)	W_{48} [4] (wt%)
Q	25.0	1890	2520	9.1
C	25.3	1940	2595	8.8
V	36.1	1550	2430	17.6

[1]porosity; [2]bulk density; [3]solid density; [4]water absorption by immersion.

The behavior of the physical characteristics was nearly the same for Q and C-mortars, as they showed similar packing density (Table 1).

The V-mortar had the highest P_w and W_{48} associated to the higher porosity of their aggregate particles, the lower particle density (Table Table *1*) and paste content. Noteworthy is the fact that V-mortar showed a bulk density about 20% lower than the remaining.

3.1.3 Water transport properties

The results of water capillary absorption, drying behavior and water vapour permeability tests are shown in Table 5 and Figure 5.

Table 5 – Water transport properties

Mortar	*WAC* [1] (kg·m^{-2}·s$^{-0.5}$)	*DI* [2]	μ [3]
Q	0.15	0.121	10.5
C	0.15	0.113	10.0
V	0.31	0.202	9.1

[1]capillary water absorption coefficient; [2]drying index; [3]water vapour diffusion resistance coefficient.

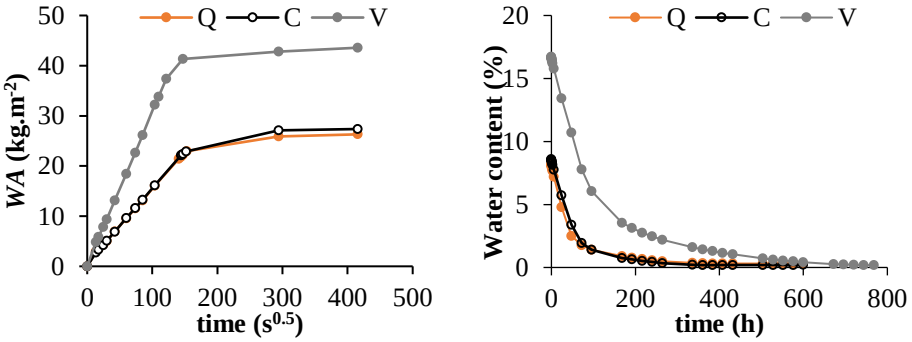

Figure 5 - Capillarity water absorption curves (left); drying behaviour curves (right).

It would have been expected that the best quality of the aggregate-paste transition zone of C-mortar would affect the water transport properties. However, the behavior was quite similar in Q and C-mortars.

The improved *ITZ* that resulted in higher mechanical strength in C-mortar (3.1.1) should be more relevant when the specimen is tensioned, affecting the weak phase of the mortar [13,24,25]. On the other hand, in tests where the specimen isn't stressed, Q-mortar benefits from having higher ϕ (and slightly lower volume of paste).

The V-mortar possessed the highest *WAC* and the lowest μ, as result of the higher porosity of the volcanic aggregate particles. Despite that, this mortar showed a higher drying period (the highest *DI*), due to the fact that it absorbed higher volume of water at the beginning of the test. In this case, the water inside the aggregates is first transferred to the paste and only then evaporates outwards, delaying drying.

3.2 Characterization of renders

3.2.1 Pull-off and surface hardness

The results of pull-of strength and surface hardness are presents in Table 6.

Table 6 - Pull-off strength and surface hardness

Rendering mortar	f_{PO}[1] (MPa)		R^2 ( )	
	masonry joint	masonry stone	masonry joint	masonry stone
Q	0.01 (N_v=2;N_i=3)	0.17 (N_v=1;N_i=0)	58±9	59±11
C	0.00 (N_v=1;N_i=4)	0.04-0.05 (N_v=2;N_i=1)	39±5	44±2
V	0.04 (N_v=1;N_i=1)	0.00-0.07 (N_v=3;N_i=1)	46±6	48±2

[1]pull-off strength: measured values, number of measurements (N_v) and number of invalid tests (N_i); [2]surface hardness (mean and standard deviation).

It should be noted that due to the low strength of mortars, there was a considerable number of invalid tests in the pull-off test, mainly due to sample detachments that occurred during the mortar cutting or equipment fixation. Therefore, the results of these two tests did not allow obtaining conclusive information about the render adhesion and could not be related with the mechanical strength of mortars prisms.

The surface hardness did not have the same tendency in mechanical strength of mortars prisms. The Q-mortar had the highest surface hardness, which was a result of the higher stiffer aggregates and lower paste volume. However, the difference between Q and C-mortar was unexpectedly high. A possible explanation for the lowest surface hardness of C-mortar may be related to the irregular surface of the render, due to the angularity of the carbonate aggregate particles [26].

It is safe to say that the results don't inform of the influence of the type of aggregate on the render adhesion to the substrate.

3.2.2 Water absorption by Karsten pipe

The water absorption by Karsten pipe test is presents in Figure 6. Three of the seven tests was performed for each mortar, were showed the fastest, the slowest and the intermediate absorption curve.

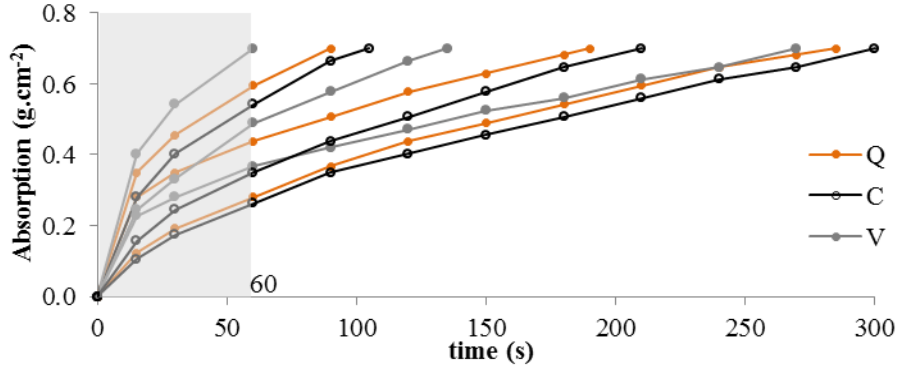

Figure 6 - Water absorption by Karsten pipe (the slowest, the fastest and the intermediate absorption for each mortar)

The results show a high variety in each type of mortar, which is a characteristic of this kind of test, and which can be a consequence of the existence of cracks and detachments in some areas of the renders [27].

The water absorption was very fast, which in all cases took less than 5 minutes, but two cases of the V-mortar took less than 60 seconds to absorb the 4ml of water. Therefore, and in order to accomplish a better comparative analyses of the mortars the first 60 seconds of test were computed. The average results of each mortar water absorption coefficient were of 0.55, 0.58 and 0.67 ($kg.m^{-2}.s^{-1/2}$) for Q, C and V-mortar, respectively. The V-mortar showed a faster absorption, which was related to its higher open porosity and the remaining mortars showed similar results. These values corroborate the tendencies that were seen in the prisms water transport characterization (3.1.3).

The differences between the results of Karsten pipe in masonry zones of the stone and joint weren't that significant, which shows that this test refers mainly to the renders surface layer.

3.2.3 Drilling resistance

In Table 7, the average values of the drilling force (F_d) are shown. They were obtained through the renders thickness and the results of several tests that were done in renders on stone and joint areas. the calculation of the average forces was made in the cases where it was possible to distinguish the interface between the render and the substrate, as well as the number of performed tests (n).

Table 7 - Drilling resistance (N)

Rendering mortar	masonry zone	mortar layer	mortar-substrate interface	n
Q	stone	5,2	0,7	3
	joint		1,2	2
C	stone	11,1	–	2
	joint		5,3	3
V	stone	7,6	–	2
	joint		–	2

For each mortar, it was selected a drilling profile which was applied on the area the stone and joint. Figure 7, 8 and 9 show these profiles for Q, C and V-mortars, respectively. The leftmost chart illustrates both tests for each mortar (masonry stone and joint) and the middle and rightmost charts show the drilling profiles alone.

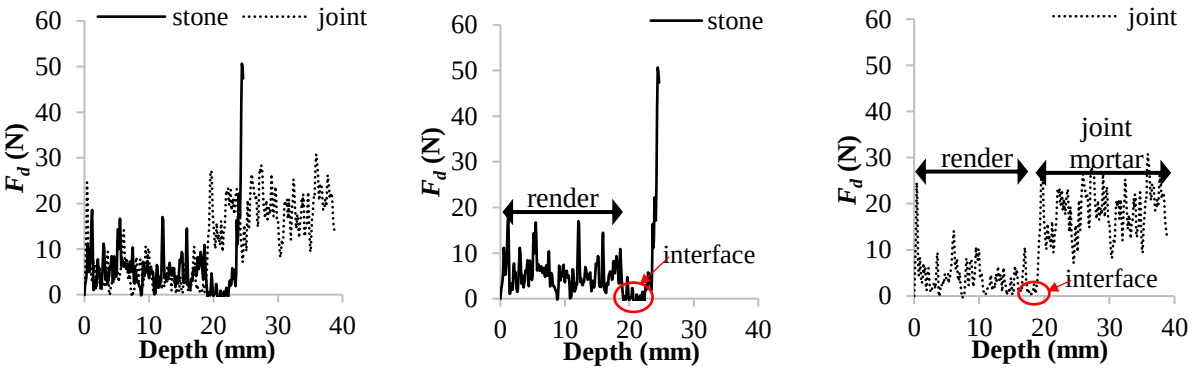

Figure 7 - Drilling profiles of Q-mortar

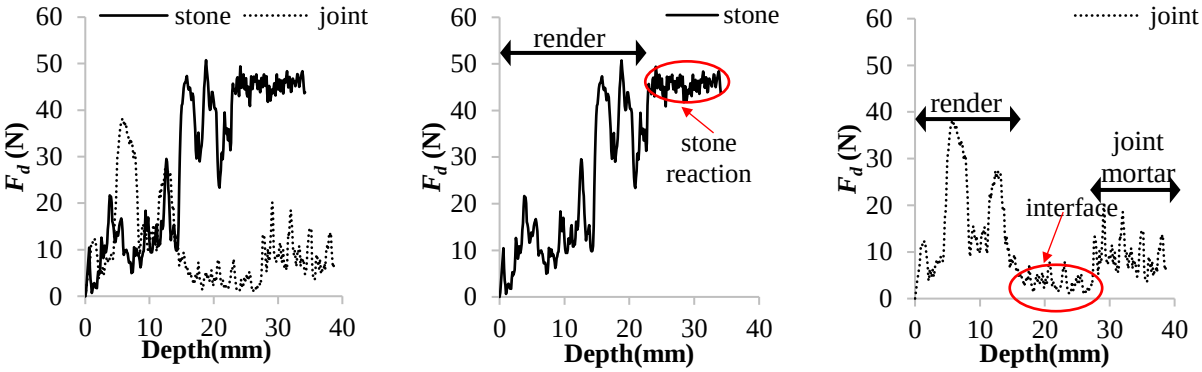

Figure 8 - Drilling profiles of C-mortar

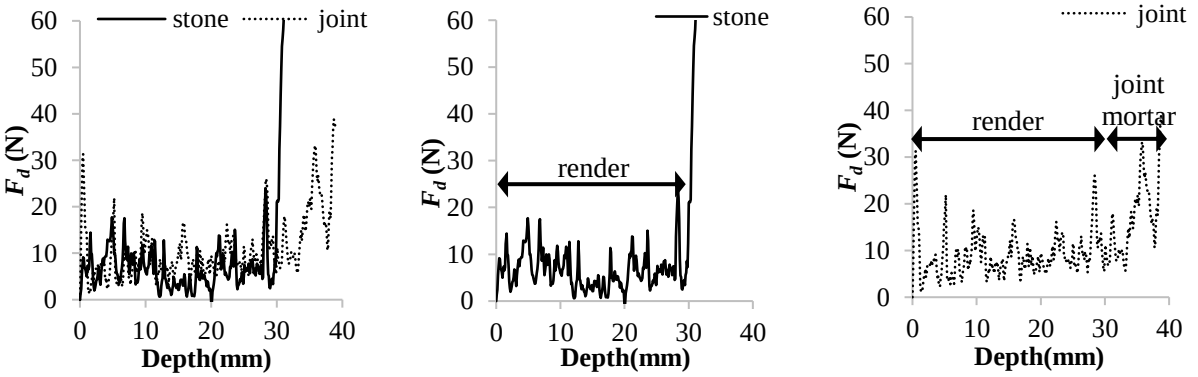

Figure 9 - Drilling profiles of V-mortar

The drilling forces verified throughout the render thickness did not change significantly when the mortar was applied on the stone and the joint, which is why the results shown on Table 7 are the results of two different situations.

The C-mortar showed a higher drilling resistance, which corroborates the results of compressive and flexural strength and the drilling resistance obtained in prisms (Figure 4-left). Nevertheless, the Q-mortar drilling resistance was very low, even when compared to the render of V-mortar. This unexpected behavior was not in accordance with the results from prisms.

The drilling resistance of mortar is as sensitive as the flexural and compressive strength as far as the stiffness of the paste and aggregates are concerned and the quality of *ITZ*. The low elastic compatibility and poor aggregate-paste bond impairs the stress transfer from the drill action, which creates a significant spread of cracks in the mortar, around the aggregate particles. On the other hand, on mortars with higher elastic compatibility, the cavity made by the drill is lower, leading to more friction between the bit and lateral surface of the hole. This phenomenon as the designation of "*package*" and originates higher drilling forces [21]. These aspects penalize the Q-mortar because of the highest aggregate stiffness and the worst aggregate-paste bond quality, which does not happen in C-mortar. The V-mortar is less affected than the Q-mortar, probably because of the better connection that exists between the aggregate-paste, which is a result to higher porosity of its aggregates and good elastic compatibility resulting from its low stiffness.

The drilling resistance tends to be higher in renders (mortar layer values, Table 7) rather than in small specimens (F_d, Table 3) of the same mortar, which can be explained in the different boundary conditions which allows higher confinement of aggregates in render [13].

The drilling behavior of the renders revealed to be an important output and is discussed below. In general, it was possible to distinguish several resistances during across the mortar-substrate interface of Q and C-mortars. The interface crossing is identified by a significant change in the drilling resistance, which takes place approximately in 20 mm of the render thickness (Figure 7 and 8). Analysing the drilling resistance interface (Table 7), the results show that the Q-mortar has a bigger adhesion to the substrate in the joint area when compared to the stone area. In C-mortar, the opposite occurs (Figure 8). Nevertheless, the expected reduction of the drilling resistance was not confirmed in the stone area. In the V-mortar, it is not possible to see a reduction of the drilling resistance in the interface (Figure 9), which suggests that the adherence to the render to the masonry support is similar to the mortar resistances.

To summarize, the adherence to the V-mortar was satisfying bearing in mind the low resistance of this mortar. In C-mortar render, the adherence to the stone area was higher, which corroborates the existence of a good connection between the lime paste and the calcite-based stone materials. The Q-mortar render seems to have developed the lowest masonry support adherence. Although the drilling resistance test results are not easy to interpret, it allowed obtaining relevant information in what regards the mortar support resistance and adherence than the pull-off test, because it is more destructive and hard-to-handle.

4 CONCLUSIONS

The results showed that the studied aggregates had affected differently the physical and mechanical behaviour of the mortars. The higher porosity and lower resistance of volcanic aggregate led to a weaker and more water-accessible mortar. It was found that the diverse mortars had different failure modes, involving the contribution of distinct mortar phases. Volcanic sand mortar was controlled by the lower mechanical strength of its aggregate particles. The mechanical strength of the quartzitic sand mortar was essentially affected by its weaker aggregate-paste *ITZ*. Mortar with carbonate aggregate could explore the maximum capacity of lime paste due to its improved aggregate-paste *ITZ*. The carbonate aggregate mortar showed the highest strength, which can be explained by the improved aggregate paste *ITZ* and the alike elastic properties of lime paste and the calcite-based aggregate. However, these are conditions mainly visible when the rupture of the material is forced, with little influence in its physical properties. Thus, mortars produced with carbonate and quartzitic sands showed similar porosity characteristics and water transport behaviour.

The characterization performed in the renders was much less informative than that obtained in prisms, showing quite scatter and somewhat erratic measurements, especially for pull-off and surface hardness tests. The pull-off test proved to be unsuitable for the weak studied mortars. While prisms are produced according to standard procedures, rendering mortars are applied, compressed and scoured manually, and thus undergoing higher variability. In addition, the masonry substrate with diverse materials (stone and mortar joints) and uneven surface may introduce further variability. Nevertheless, the water absorption from the Karsten pipe test corroborated the water absorption results obtained in prisms.

Drilling resistance test was considered the most informative of the *in situ* characterization tests. It provided the mechanical resistance of the rendering mortars and the renders adhesion to the substrate.

REFERENCES

[1] Cavaco L.S.R., *Técnicas de aplicação de argamassas de revestimento em edifícios antigos. Influência no desempenho*, Lisboa, IST, 2005.

[2] Moropoulou A., Bakolas A., Moundoulas P. and Aggelakopoulou E., *Reverse engineering: a proper methodology for compatible restoration of mortars*, RILEM Publications, pp. 278-291, 2009.

[3] Veiga M.R., *Argamassas para revestimento de paredes de edifícios antigos. Caracteristicas e campo de aplicação de algumas formulaçoes correntes.* Actas do 3º Encore, Lisboa, LNEC: Encontro sobre Conservação e Reabilitação de edifícios, pp. 1-10, 2003.

[4] Veiga M.R. and Carvalho F., *Argamassas de reboco para paredes de edificios antigos: requisites e caracteristicas a respeitar.* LNEC: Cadernos de Edificios, nº2, pp. 39-55, 2002.

[5] RILEM TC 203-RHM, *Repair mortars for historic masonry. Performance requirements for renders and plasters.* Mater.Struct., Volume 45, p. 1277-1285, 2012.

[6] Veiga M.R., *Argamassas na conservação.* Actas das 1ªs Jornadas de Engenharia Civil da Universidade de Aveiro, Lisboa, LNEC, pp. 1-22, 2003.

[7] Stefanidou M. and Papayianni I., *The role of aggregates on the structure and properties of lime mortars*, Cem.Concr.Compos., 27, 914–919, 2005.

[8] Nogueira R., Ferreira Pinto A. and Gomes A., *Rebocos á base de cal: passado e presente. Conhecimento empírico versus conhecimento científico*, In Proceedings of the V Jornadas FICAL, Fórum Ibérico da Cal, Lisboa, LNEC, 2016.

[9] Feret R., *About the compacity of hydraulic mortars (in French: Sur la compacite des mortiers hydrauliques*, C. Dunod, Paris, 1892.

[10] Rato V., *Influence of the morphological microstructure on the mortar behavior*. Ph.D. Thesis, New University of Lisbon (in Portuguese). Lisbon, 2006.

[11] Lanas J. and Alvarez J., *Masonry repair lime-based mortars: factors affecting the mechanical behavior*, Cem.Concr.Res., 33(11), 1867-1876, 2003.

[12] Gleize P., Muller A. and Roman H., *Microstructural investigation of a silica fume-cement-lime mortar*. p. 25: 171-175, 2003.

[13] Nogueira R., Pinto A. and Gomes A., *Assessing mechanical behavior and heterogeneity of low-strength mortars by the drilling resistance method.*, Constr.Build.Mater., 68, 757–768, 2014.

[14] Fragata A. and Veiga R., *Air lime mortars: The influence of calcareous aggregate and filler addition*. Mater.Sci.Forum, 636-637, 1280-1285, 2010.

[15] Scannell S., Lawrence M., Walker P., *Impact of aggregate type on air lime mortar properties, 6th International Conference on Sustainability in Energy and Buildings, SEB-14*, Energy Procedia, 62, 81-90, 2014.

[16] Santos A., Veiga R., Santos Silva A. and Brito J., *Influence of the aggregates' nature and particle size distribution on the mechanical properties of lime based mortars*, In proceedings of the 4th Historic Mortars Conference (HMC16), Santorini, 2016.

[17] Mangulkar M.N., *Review of particle packing theories used for concrete mix proportioning*, Int.J.Sci.Eng.Res., 4(5), 143-148, 2013.

[18] Mosquera M., Silva B., Prieto B. and Ruiz-Herrera E., *Addition of cement to lime-based mortars: Effect on pore structure and vapor transport*, Cem.Concr.Res., 36, 1635–1642, 2006.

[19] Nogueira R., Ferreira Pinto A. and Gomes A., *Water behaviour of a lime mortar treated with consolidants*, Proceedings of the 3rd Historic Mortars Conference, 63-70, Glasgow, 2013.

[20] Bogas A., *Caracterização de betões estruturais com agregados leves de argila expandida*, Dissertação de Doutoramento em Engenharia Civil: IST, Lisboa, 2011.

[21] Nogueira R. "Lime plasters and renders: characterization and assessment of consolidation treatments", Ph.D. Thesis, Instituto Superior Técnico, Universidade de Lisboa, Lisboa, 2016.

[22] Mindess S., Young J. and Darwin D., *Concrete*, 2nd ed., Prentice Hall. Pearson Education, Inc., 2003.

[23] Bogas J.A., Gomes M.G. and Real S., *Capillary absorption of structural lightweight aggregate concrete*. Mater.Struct., 48(9), 2869-2883, 2014.

[24] Van Mier J. and Vervuurt, A., *Test Methods and Modelling for Determining the Mechanical Properties of the ITZ in Concrete*, Proceedings of the Engineering and Transport Properties of the Interfacial Transition Zone in Cementitious Composites, RILEM, 19-52, 1999.

[25] Neville A. *Properties of Concrete*, 5th ed., Prentice Hall, UK, 2012.

[26] Katz O., Reches Z., Roegiers J.-C., *Evaluation of mechanical rock properties using a Schmidt Hammer*, Int.J.Rock Mech.Min.Sci., 37**,** 723-728, 2000.

[27] Duarte R., Colen I. and Brito J., *In situ testing techniques for evaluation of water penetration in rendered facades - The portable moisture meter and karsten tube*, Proceedings of the XII DBMC, Porto, Portugal, 2011.